NUMERICAL ANALYSIS OF SOILBAGS UNDER COMPRESSION AND CYCLIC SHEAR

Yousef Ansari[1], Richard Merifield[1], Haruyuki Yamamoto[2] and Daichao Sheng[1]

[1]Centre for Geotechnical and Materials Modelling, The University of Newcastle, Callaghan, NSW 2308, Australia

[2]Graduate School for International Development and Cooperation, Hiroshima University, 1-5-1 Kagamiyama, Higashi-Hiroshimashi, 739-5829, Japan

ABSTRACT

This paper presents a finite element model for analysing the behaviour of granular material wrapped with polyethylene bags under vertical compression and cyclic shearing. The simple Mohr-Coulomb model is used to represent the soil behaviour. The polyethylene bag is represented by a linear-elastic-perfect-plastic model. The soil-bag interface is modelled with contact constraints. The main purpose of the numerical analysis is to validate the anticipated performance of soilbags under various loading conditions and hence the effectiveness of soilbags as a method of ground improvement.

INTRODUCTION

Soilbags or sandbags, "Donow"s in Japanese, continue to be used to construct either temporary or permanent structures and are bags filled with granular materials like sand, crushed stone, or recycled concrete. Two significant characteristics can be associated with these soilbags (Aqil et al. 2006a): (1) their ability to convert the negative effects of external loads in a positive manner which is referred to as the "reversal idea" in the mechanism of soilbags, and (2) their ability to transform frictional materials to cohesive-frictional materials showing an apparent cohesion. In other words, granular soils wrapped with bags exhibit the typical characteristics of cohesive-frictional materials (Matsuoka et al. 2001). These mechanisms have encouraged geotechnical engineers to consider soilbags as a cheap, environmental friendly and convenient alternative for soil reinforcement.

The rapid deterioration of soilbags when exposed to prolonged ultraviolet rays confined their application solely to temporary structures such as embankment lifting, flooding barriers, or as short-term construction materials aiding reconstruction works after disasters. While the use of soilbags for temporary purposes has been established for a long time, its use in permanent constructions through quality-controlled soilbags (Solpack) is rather new. Quality-controlled soilbags are constructed by wrapping soils in particular bags. Some distinctive features of these solpacks include: making use of high-quality bags (e.g., Polyesters or Polypropylenes), selection of higher-quality filling materials along with optimising the quantity of filling materials, appropriate arrangement of the soilbag, and preloading soilbags during constructions (Matsuoka and Liu 2003).

Previous research on the application of solpacks has included their use as reinforcement for increasing the bearing capacity of soft soil foundations (Matsuoka and Liu 2003; Matsuoka et al. 2001), as damping layers for the vibration reduction transmitted from traffic loads (Matsuoka and Liu 2006), as facings installed in front of geosynthetic-reinforced soil retaining walls (Tatsuoka et al. 1997), and as ballast foundations of railway tracks for access roads in mountainous areas. More recently, soilbags, due to their significant compressive strength, have been used successfully to construct arch structures to support embankments (Kubo et al. 2001).

Soilbags have already been applied to reinforce truck roads in Nagoya City, Japan, with asphalt & concrete pavements or as reinforcement for soft building foundations to improve the bearing capacity of footings as well as to reduce traffic-induced vibrations (Matsuoka 2003; Matsuoka and Liu 2003). Other field applications include frost heave prevention (Suzuki et al. 2000) in the Hokkaido area, Japan.

The mechanical behaviour of a single soilbag under vertical compression has been investigated by Matsuoka and Liu who also proposed a simplified analytical model. The proposed method was validated through biaxial compression and unconfined compression tests. Simplifying assumptions of this analytical model are:

1. The filling material is cohesionless,
2. The filling material is assumed weightless,
3. The soilbag has a rectangular cross section,

4. Plane strain conditions are assumed,
5. Soil and bag interfaces are frictionless (free relative horizontal displacement between soil and bag is likely),
6. The change in the thickness of the membrane is neglected,
7. The principal stress ratio of the soil is assumed to follow an exponential function; and
8. The volumetric strain of the soilbag is neglected (based on experimental results).

Friction along the contact surfaces of bags, soilbags with different filling materials, and soilbags lying on different base materials has also been experimentally investigated by means of a series of laboratory shear tests (Matsuoka and Liu 2006). Average initial and peak frictional coefficients for various contact interfaces were obtained. The results show that frictional angle due to horizontal loading of soilbags is dependent on the filling-material grain size as a result of local angularity. Maximum horizontal resistance of soilbags resting on top of other soilbags is shown to be directly proportional to the inclination angle of that soilbag. It is also illustrated that horizontal sliding resistance of soilbags could significantly be increased by bedding in concrete slabs between soilbags and rockfill base materials.

Yamamoto et al (2003) performed some laboratory cyclic simple shear tests on soilbags filled with Silica sand to evaluate their vibration reduction potential. In their studies they introduced an "equivalent damping ratio" as a function of energy loss in one cyclic load divided by the total elastic strain energy. The equivalent damping ratio for the assembly of soilbags was much higher than those of both the concrete structures and steel structures by a ratio of 6 and 15, respectively. Accordingly, solpacks have been suggested to be used as vibration absorbers in order to reduce traffic-induced vibrations (Matsuoka and Liu 2003).

Lohani et al (2006) investigated the effects of soilbag materials, backfill soil type, and number of soilbags on compression strength and shear strength in a soilbag-pile. It was concluded that the initial compaction of soilbags and preloading effectively decrease the creep deformation and favourably increase the initial stiffness of the bags. In addition, results of lateral shear tests revealed that the shear strength of a soilbag

pile is substantially smaller compared to its compression strength. Low initial stiffness of virgin soilbags during relatively small compression is introduced as one drawback of soilbag-piles. Subsequently, Matsushima et al (2008) showed that a pile of soilbags is much less stable when sheared laterally than when compressed vertically.

Although numerous studies related to field and laboratory tests on soilbags can be found in literatures, numerical studies of soilbags under different loading circumstances is relatively few. Numerical analysis can be used to validate the anticipated behaviour of soilbags under complex loading conditions. This must have been caused by complexities arising from simulating the real geometry of a soilbag plus imposing real soilbag assembly constraints.

In (Muramatsu et al. 2007), a numerical analysis of the ground reinforced by soilbags has been conducted by applying an elasto-plastic finite element analysis (FEA). The soilbags in the ground are represented by truss elements. Finite deformation is considered in the analysis due to the occurrence of large deformations in the model tests. The numerical results show good agreement with two-dimensional model tests on aluminium rods, both qualitatively and quantitatively. Muramatsu et al. (2009) further evaluated the damping effects of soilbags against vibration via numerical simulation. Again, soilbags are represented by truss elements. The t_{ij} model proposed by Nakai and Hinokio (2004) was used to represent the soil behaviour. The simulated results seem to verify the effectiveness of soilbags as a vibration damping material. More recently, Tantono and Bauer (2008) conducted numerical analysis of a sandbag under vertical compression. They used a hypoplastic model to represent the sand in the bag and a linear-elastic-perfect-plastic to model the bag. The bag is modelled with membrane elements. Frictionless and interlocked interfaces between soil and bag have been considered and the evolution of the tensile force within the bag has been investigated for both scenarios. The numerical results seem to verify the behaviour of soilbags under compression.

In this study, a finite element model is presented for analysing the behaviour of granular material wrapped with polyethylene bags under vertical compression and cyclic shearing. The simple Mohr-Coulomb model is used to represent the soil behaviour. The polyethylene bag is represented by a linear-elastic-perfect-plastic

model. The soil-bag interface is modelled with contact constraints. The main purpose of the numerical analysis is to validate the anticipated performance of soilbags under various loading conditions and hence the effectiveness of soilbags as a method of ground improvement.

FINITE ELEMENT MODEL FOR SOILBAG

Soil Behaviour

The behaviour of frictional soil is represented by a non-associated Mohr-Coulomb model. More advanced models could have been used. However, the main purpose of the analysis here is to study the behaviour of a soil-bag assemblage. It is deemed beneficial to investigate what can be achieved with a simple and perhaps most commonly used soil model. The Mohr-Coulomb model has a rounded yield surface on the deviatoric plane using the $M(\theta)$ method (Argyris et al. 1974); (Sheng and Sloan 2000). Again, more advanced methods such as the Matsuoka and Nakai (1974) or the Lade and Duncan (1975) method could be used, but would not lead to significant difference in the numerical results. The Mohr-Coulomb model is implemented in the commercial FEM code ABAQUS and it is a matter of convenience to use this model to represent the behaviour of the frictional material. The material properties involved in this model are:

1. The angle of internal friction of the soil, ϕ'
2. The angle of dilation of the soil, ψ'
3. The elastic Young's modulus, E'
4. The Poisson ratio, υ
5. The cohesion of the soil, c'

Bag Material

The bag material is modelled with a linear-elastic-perfect-plastic von Mises model. The material parameters involved in this model are:

1. The elastic Young's modulus, E
2. The Poisson ratio, υ
3. The tensile strength, c

Soil-Bag Interface

One difficulty in simulating real behaviour is that loads applied to the assembly of a soilbag have to be transferred between soil and bag primarily through contact of surfaces. One possible solution to this intricate loading condition is to use interface or joint elements where a normal and tangential stiffness are used to model the pressure transfer and friction at the interfaces. Such elements can have a very small or even zero thickness, but can not be used for large interfacial displacements or surface separation and reclosure.

An alternative approach for modelling interfacial contact problems between two solid bodies is to use contact kinematic constraints which take into account nonlinearities due to large deformations, surface separation and reclosure. Applications of contact elements into Geomechanics refers to, e.g. (Sheng et al. 2006).

In the finite element analysis in this paper, contact elements are used to model the soil-bag interaction. The simple Coulomb friction law is used to define the friction between the soil and the bag:

$$\begin{aligned} &g_T = 0, \text{ when } \mu t_N - |t_T| > 0 \longrightarrow \text{(stick state)} \\ &|g_t| > 0, \text{ when } \mu t_N - |t_T| = 0 \longrightarrow \text{(slip state)} \\ &g_t(\mu t_N - |t_T|) = 0 \end{aligned} \tag{1}$$

where g_t is the relative displacement in the tangential direction at the interface, t_T is the tangential stress at contact, and μ is the coefficient of friction.

Normal forces at contacts are transferred via a simple constraint:

$$\begin{aligned} &g_N = 0, \text{ when } t_N > 0 \\ &g_N > 0, \text{ when } t_N = 0 \\ &t_N g_N = 0 \end{aligned} \tag{2}$$

where g_N is the relative displacement in the normal direction (or the normal gap), and t_N is the normal stress at the contact.

The normal and tangential gaps are computed from the displacements. The normal and tangential stresses are then related to the normal and tangential gaps, respectively, via the penalty method (Wriggers 2002). The only parameter involved in the contact constraints is the interfacial friction μ.

Finite Element Code

There are several commercial packages that can be used to analyse large deformation contact mechanics problems. ABAQUS is one of these codes and it has some reasonable constitutive models for geomaterials. Sheng et al (2005) used 'ABAQUS' to simulate the installation and loading of displacement piles. The corresponding numerical results have been compared with measured values from centrifuge tests. Merifield (2008) reported the results of finite element analyses of shallowly embedded pipelines under vertical and horizontal load using 'ABAQUS'. Randolph et al (2008) also used 'ABAQUS' to investigate the large geometric changes associated with near-surface penetration or breakout of anchors and other large deformation problems. We are also using ABAQUS here to analyse the behaviour of soilbags.

Material Properties

The problem mainly focuses on the evolution of stress and deformation in a soilbag assembly under monotonic vertical loading and cyclic shear loading conditions. Numerical analyses are carried out for both two-dimensional (2D) and three-dimensional (3D) models. A 3D analysis was necessary in order to model thin surface of the wrapping material with membrane elements. Both models take into account the contact boundary conditions at the soil-bag interface. Accordingly, large frictional sliding, surface separation and reclosure at the soil-bag interfaces are permitted.

Ordinary polyethylene (PE) bags are considered. In the first scenario, the soilbag is subjected to an unconfined vertical compression while the second scenario deals with the cyclic horizontal shearing of a soilbag.

The wrapping PE material has a thickness of 0.1 mm. It is considered as a linear-elastic-perfect-plastic material with the following properties: Young's modulus (E) of 500 MPa, Poisson's ratio (υ) of 0.3, yield stress (σ_y) of 100 MPa. These values are typical for PE bag materials according to (Matsuoka and Liu) (2006).

The granular material was modelled as a non-associated Mohr–Coulomb material with the following properties: Young's modulus (E) of 100 MPa, Poisson's ratio (υ) of 0.3, internal friction angle of 40°, dilation angle of 5~15°, and cohesion (c) of 1 kPa. These material properties are typical for dense sands or gravels (Lambe and Whitman 1979). The small cohesion is used to avoid numerical instability.

The friction coefficient between the soil and the bag is assumed to be 0.84, which is equivalent to the internal friction angle of the soil (tan (40°)=0.84). The bag and the soil are allowed to separate whenever the contact normal stress becomes negative (tension).

FE Mesh for Soilbag under Compression

Three-dimensional numerical simulation of a 80 cm × 40 cm × 10 cm soilbag under unconfined vertical compression is carried out in order to study the behaviour of the soilbag under a vertical compressive load. To minimize the calculation times, the symmetrical geometry of the soilbag is used and accordingly, only a quarter of the soilbag is modelled. The finite element meshes for the assembly of a soil-bag are shown in Fig. 1. The assembly consists of a rigid loading panel, the wrapping bag and the soil inside (Fig. 2). The rigid loading panel is used to ensure that the top surface of the soilbag remains flat during the loading process. A uniform vertical displacement is applied to the loading panel over a number of increments. The width of the loading panel is sufficiently large so that the soilbag will not be squeezed out of the loading panel even after large deformation.

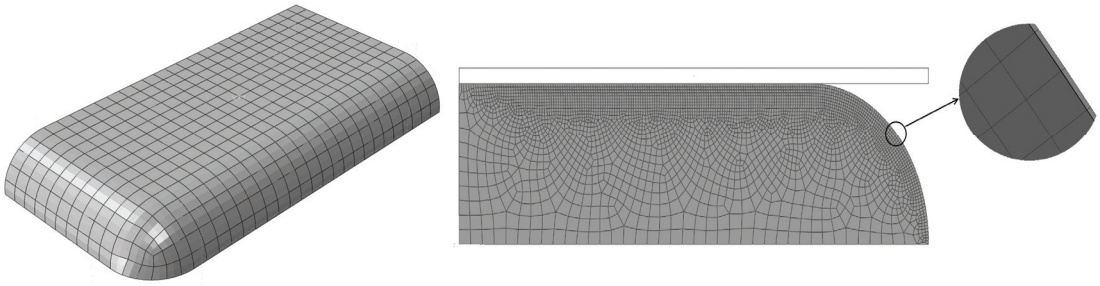

(a) Three-dimensional (b) Two-dimensional

Fig 1. Initial geometry and finite element mesh of the soilbag assembly.

In the three-dimensional model, the bag and the soil are discretised into uniformly distributed elements. The soil is represented by 8-noded linear 3D elements (C3D8), whilst the bag by 4-noded quadrilateral membrane (M3D4) elements. The main characteristics associated with the plane stress membrane elements are the insignificant bending and transverse shear stiffness. The loading panel is assumed to be a rigid body and meshed accordingly. Figure 2 illustrates the parts required in the assembly of a soilbag. In the 2D model, 4-node plane strain quadrilateral elements (CPE4) are used both for the soil and the bag. The elements for the soil are refined while approaching the soil-bag interface as shown in Fig. 1b. The elements for the bag are very fine, due to the small thickness (0.1 mm) of the bag.

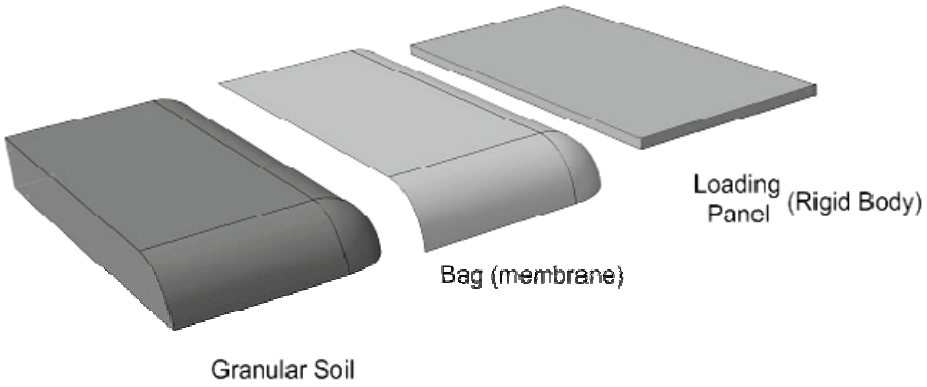

Fig 2. Main parts for the assembly of a soilbag (3D Model).

For the problem presented, two distinct contact interfaces are defined to model the soil/bag and bag/loading panel interactions: the soil/bag interface is modelled using the surface-to-surface finite-sliding formulation with the concept of master surface (soil) and slave surface (bag), and the bag/loading panel interface is modelled via node-to-surface finite-sliding formulation using master (loading panel)/slave (bag) approach as formulated in ABAQUS. The master and slave surfaces are defined as shown in Fig. 3. The elements in the soil and bag domain that are initially in contact are defined as interacting surfaces. However, for the loading panel/bag contact, those nodes with the possibility of contact during the analysis are selected as interacting node regions. This allows the possibility of elements on the bag surface coming into contact with the loading panel as the analysis progresses. For soil/bag contact interaction using a surface to surface discretisation method, an automatic smoothing is applied to contacting surfaces in order to reduce inaccuracies in contact pressures

caused by mesh discretisation on curved geometries of a soilbag with lateral boundaries. Details of interacting surfaces are presented in Table 1.

Table 1. Details of the surface interactions for the assembly of a soilbag.

Feature / Interface	Soil-Bag	Bag-Loading Plate
Discretisation Method	*surface to surface*	*node to surface*
Tracking approach	*Finite sliding*	*Finite sliding*
Constraint enforcement method	*Penalty method*	*Penalty method*
Surface smoothing	*Yes*	*No*

The contact between the bag and the loading panel also follows the Coulomb friction law with a coefficient of friction of 0.5. In order to establish a uniform loading condition throughout the analysis, no surface separation is allowed during loading steps.

The numerical analysis is carried out in 2 individual steps. The first step of the analysis establishes the initial contacts between the loading panel and the bag and between the bag and the soil. The vertical compression is applied during the second step.

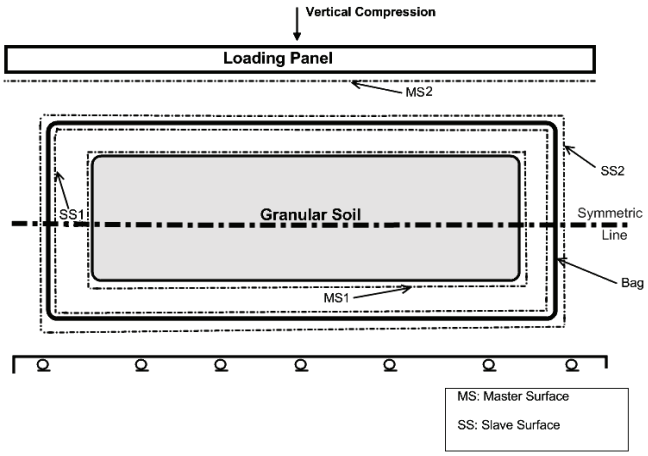

Fig. 3. Geometry and boundary conditions for the assemblage of soilbag.

The soil is assumed weightless throughout the numerical simulation. The boundary conditions are shown in Fig.3. Because the problem involves various nonlinearities (material, boundary conditions and large deformation), numerical convergence is a challenge and very fine time steps have to be used.

FE Mesh for Soilbag under Cyclic Shearing

In this part, a 80 cm × 40 cm × 10 cm soilbag is subjected to cyclic simple shear and its mechanical behaviour is investigated through two- and three-dimensional numerical simulation. Assuming the mid-plane of the soilbag remains stationary during the shear test, we consider half of the soilbag. The geometry and finite element meshes are shown in Fig. 4. Mesh and element types assigned to the two- and three-dimensional model for this scenario is very similar to those of the case of vertical compression (Fig. 2a), with the soil represented by 8-noded linear elements and bag by 4-noded membrane elements. Since the soil has a small dilation angle and its volume may increase to some extent during the shear test, quadratic elements are used here instead of linear elements. Quadratic elements are generally considered to be better than linear elements for incompressible or dilatant materials, even though numerical tests for the problem studied here show very little difference in the results. Cyclic horizontal displacement is applied to the loading panel over a number of increments. Again, the width of loading panel is made sufficiently large that the soilbag will not be sheared outside the panel even after large deformation.

Three-dimensional Two-dimensional

Fig. 4. Initial geometry and mesh of the assembly of a soil-bag under cyclic shear.

The analysis is carried out in 3 steps: the first step to establish the contact interactions between interfaces, the second step to apply a monotonic vertical compression on the load panel and the third step to apply cyclic horizontal displacements to the loading panel. To ensure the shear is applied to the soilbag, a relatively high coefficient of friction between the loading panel and the bag ($\mu = 0.99$) is used.

The boundary conditions for the cyclic simple shear test are similar to those shown in Fig. 3, except that the horizontal movement at the mid-plane (symmetric line in Fig. 3) is not allowed during the last step. A surface-to-surface finite sliding master/slave contact is chosen to define the soil/bag interface. In this simulation, a 'path-based' tracking algorithm has to be considered to model the membrane with double-sided contact surfaces. The 'path-based' tracking algorithm is the only algorithm that allows for double-sided master/slave contact surfaces. The automatic smoothing is also enabled due to the semi-circular boundaries of the soilbag.

NUMERICAL RESULTS

Mechanical Behaviour of a Soilbag under Vertical Compression

The numerical load-settlement relationship of a three-dimensional soilbag experiencing unconfined compression for (a) different soil types, and (b) different bag thicknesses are illustrated in Fig.6. As shown, a comparison between the compression behaviour of the granular material and the soilbag indicates a dramatic increase in the stiffness and the compression capacity of the assembly of soilbag. Fig.7 and Fig.8 show filled contours of the measured stress components inside a soilbag structure in an arbitrary time step.

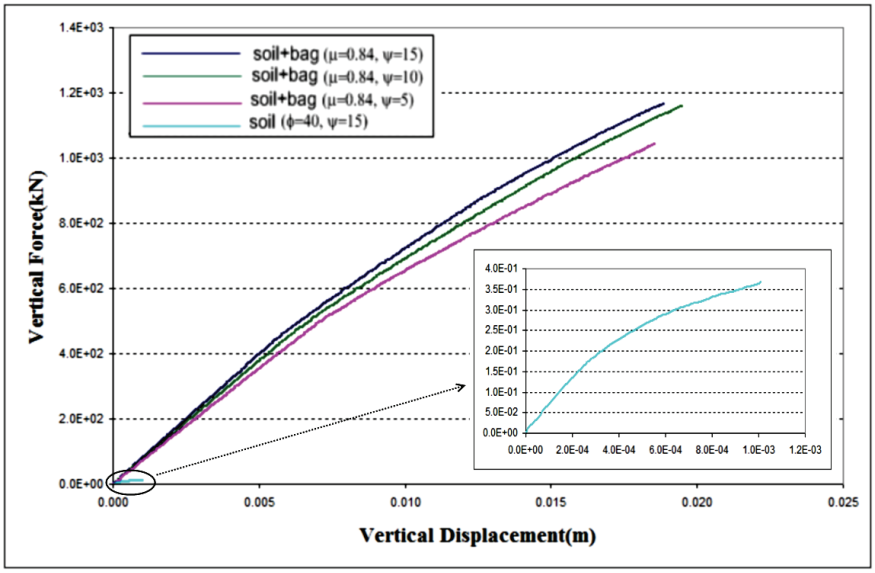

(a)

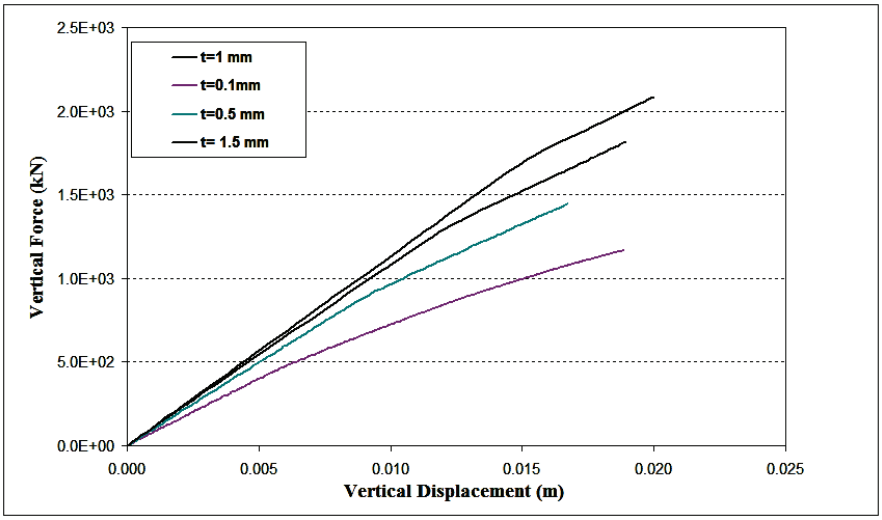

(b)

Fig 6. Load-displacement relationship for a 3D assembly of soilbag under vertical compression for (a) different soil types, (b) various bag thicknesses.

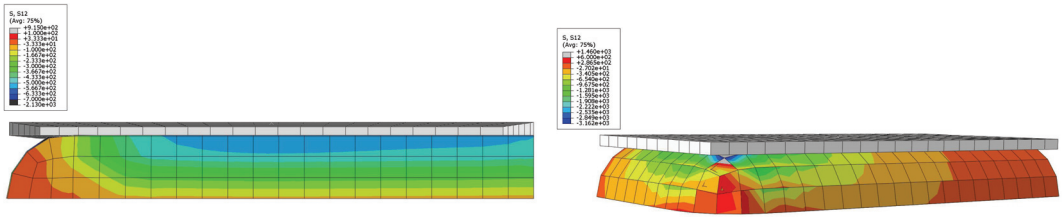

(a) Soil (b) Bag

Fig 7. Filled contours of measured stress component S12 (shear stress) within (a) the soil, and (b) the bag under vertical load (unit: kPa)

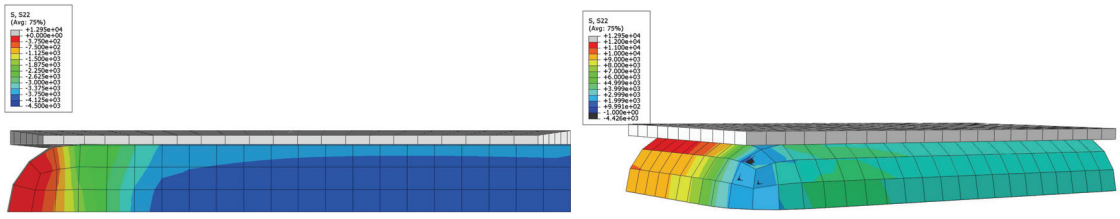

(a) (b)

Fig 8. Filled contours of measured stress component S22 (vertical stress) within (a) the soil, (b) the bag under vertical load (unit: kPa)

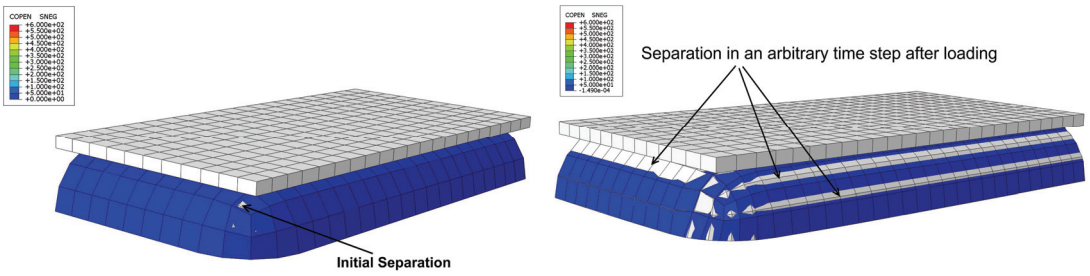

(a) Initial separation (b) Separation during loading

Fig 9. Separations at the soil-bag interface (a) prior to, and (b) after compression loading.

Two dimensional numerical analysis of a soilbag subject to vertical compression load and cyclic simple shear load are also obtained which provide more convenient outputs to investigate local separation as well as evolution of stresses within the soilbag. Fig.10 shows the evolution of tensile force within the bag for a three-dimensional sandbag under vertical compression.

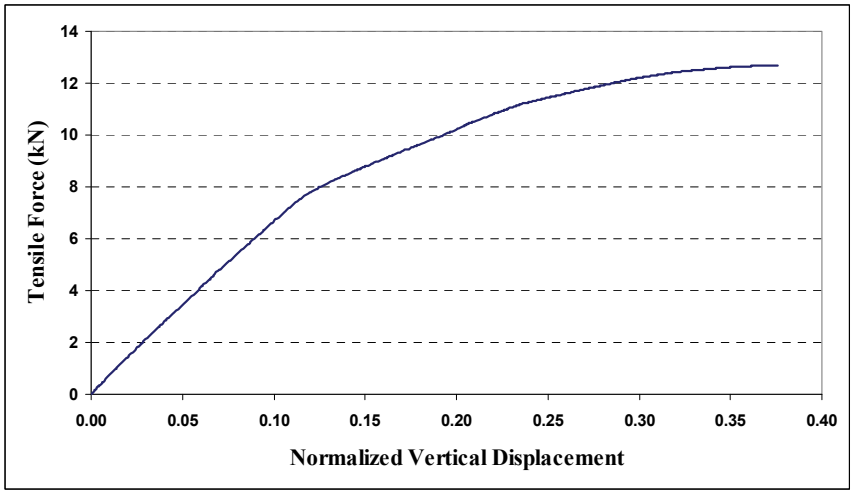

Fig 10. Evolution of the tensile force within a bag during vertical compression.

Mechanical Behaviour of a Soilbag under Cyclic Shear Test

The numerical horizontal loading-displacement relationship of a soilbag undergoing cyclic simple shear test is shown in Fig.11. Local separation at the soil-bag interface

during an arbitrary cyclic shear test is illustrated in Fig.12. Fig.13 & Fig.14 represent the filled contours of measured stress components within a soilbag in an arbitrary time step.

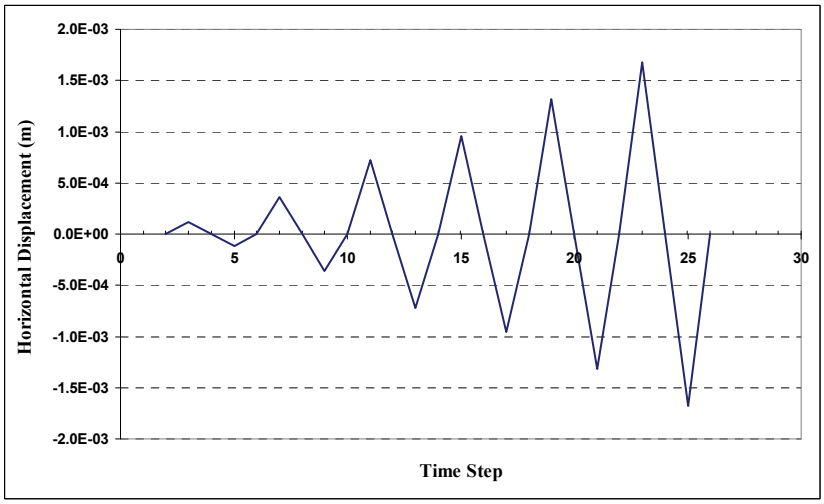

(a)

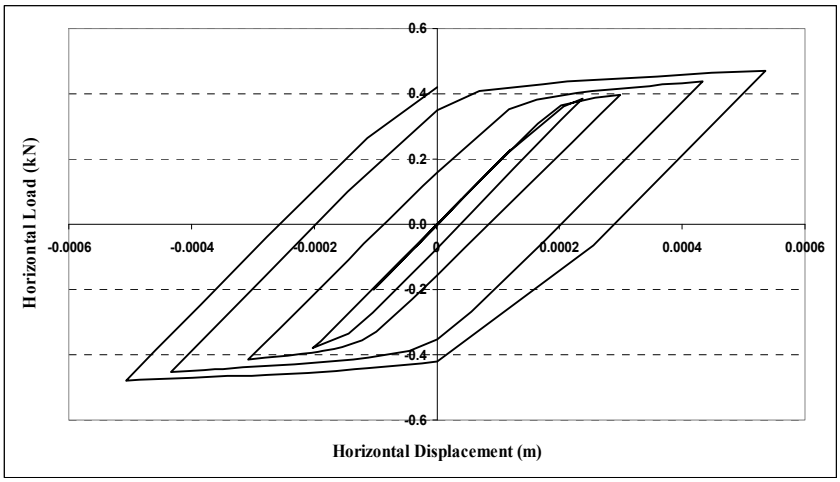

(b)

Fig 11. (a) Applied lateral loading, and (b) Typical hysteretic load–displacement curves for a 3D soilbag under cyclic shear.

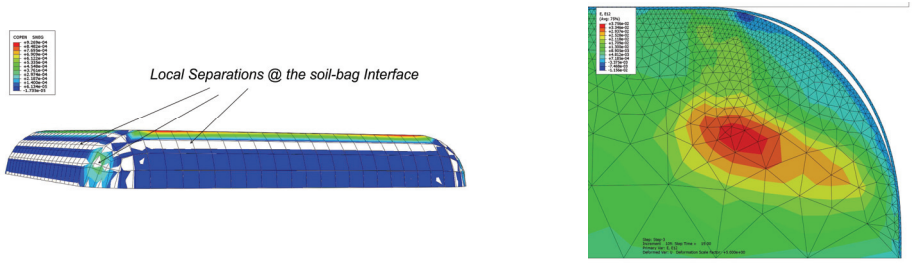

3D Model 2D Model

Fig 12. Local separation-reclosure at the soil-bag interface during the cyclic shear test.

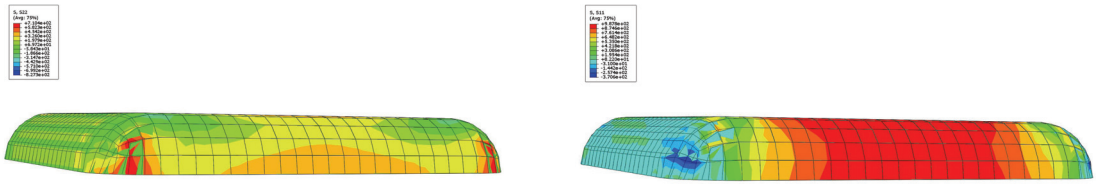

(a) Vertical Stress (S22) (b) Horizontal stress (S11)

Fig 13. Filled contours of measured stress components within the wrapping material (unit: kPa)

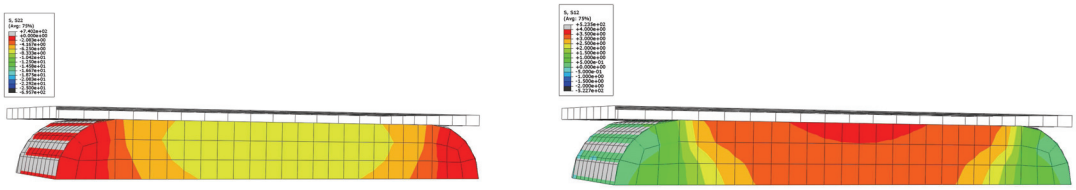

(a) Normal Stress (S22) (b) Shear stress (S12)

Fig 14. Filled contours of measured stress components within the granular material (unit: kPa)

Application of soilbags as vibration-reducing structural elements necessitates a study on the energy absorption potential within a soilbag throughout a cyclic simple shear test. The energy balance equation of the entire soilbag under cyclic shear test can be written as:

$$E_I + E_V + E_{FD} - E_W = E_{total} = \text{constant} \tag{7}$$

and,

$$E_I = E_E + E_{PD} + E_{VE} \tag{8}$$

where E_I is the internal energy; E_V and E_{FD} define the energies dissipated by damping and frictional contact mechanisms, respectively; E_W is the work done by the externally applied loads; and E_E , E_{PD}, and E_{VE} represent elastic dissipated strain energy, inelastic dissipated energy, and viscoelasticity dissipated energy, respectively.

The evolution of the different energy components in a soilbag assembly (with the friction coefficient of 0.84) while subjected to a cyclic shear test is presented in Fig.15. Evolution of frictional dissipation (E_{FD}) defines the fraction of the frictional work mainly converted to heat among contacting surfaces. Heat is instantaneously distributed among each of the contacting bodies by conduction and radiation while no heat capacity is considered for the contact interface.

In the coupled thermal-mechanical surface interactions, the rate of frictional energy dissipation is given by:

$$P_{fr} = \tau_{cr} \cdot \dot{\gamma} \tag{9}$$

And

$$\tau_{cr} = \sqrt{\tau_1^2 + \tau_2^2} \tag{10}$$

Where τ_{cr} is the critical frictional stress, τ_1 and τ_2 are active shear stresses on the contacting surface, and $\dot{\gamma}$ is the slip rate. The portion of this energy released as heat on master surface A and slave surface B would be:

$$E_{FD(A)} = f \cdot \eta \cdot P_{fr}$$

and (11)

$$E_{FD(B)} = (1-f) \cdot \eta \cdot P_{fr} \tag{11}$$

Where η is the fraction of dissipated energy converted to heat (ABAQUS default value is 1.0), and f is the weighting factor which defines the distribution of heat between contacting bodies (= 0.5). Fig.16 shows the numerical results of the evolution of E_{FD} inside a sandbag for different friction coefficients between soil and bag interface. As illustrated, E_{FD} increases with the decrease in the value of friction

coefficient (μ) as a result of the increase in the slip rate ($\dot{\gamma}$). Conversely, the inelastic dissipation energy of a soilbag assembly demonstrates a completely different trend with any increase in the value of μ (Fig.16(b)).

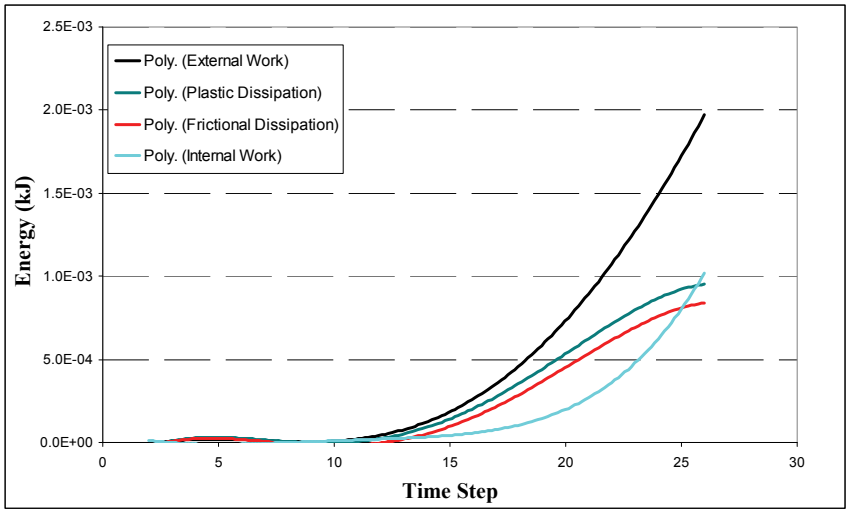

Fig 15. Evolution of energy components within a soilbag during cyclic shear test.

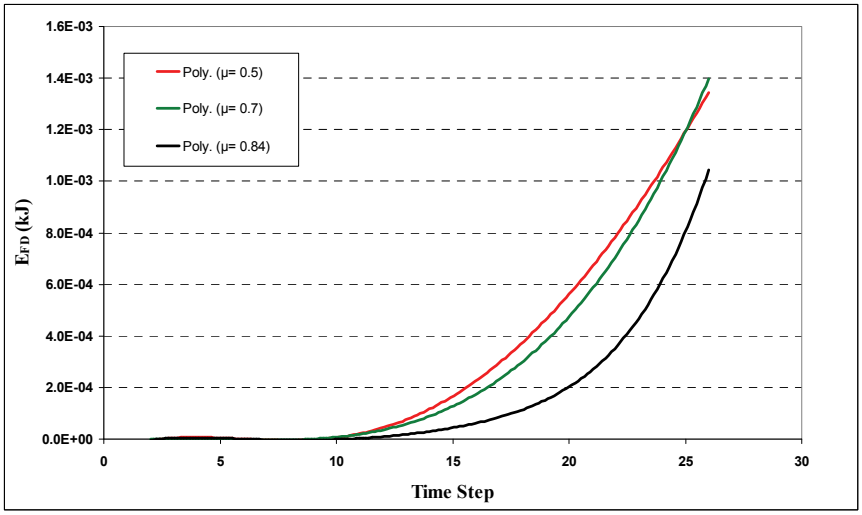

(a)

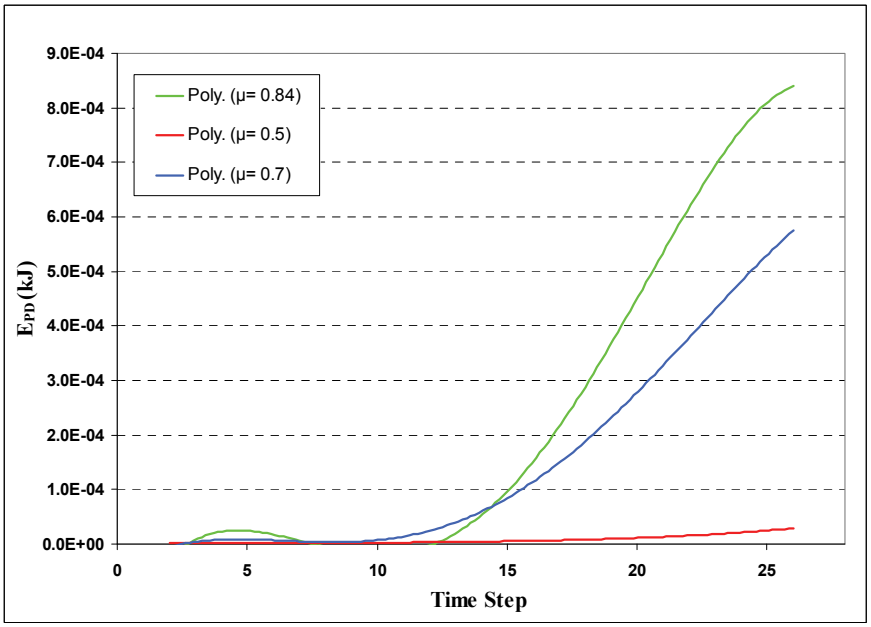

(b)

Fig 16. Comparison of the evolution of (a) frictional dissipation energy, and (b) inelastic dissipation energy within a soilbag during cyclic shear test.

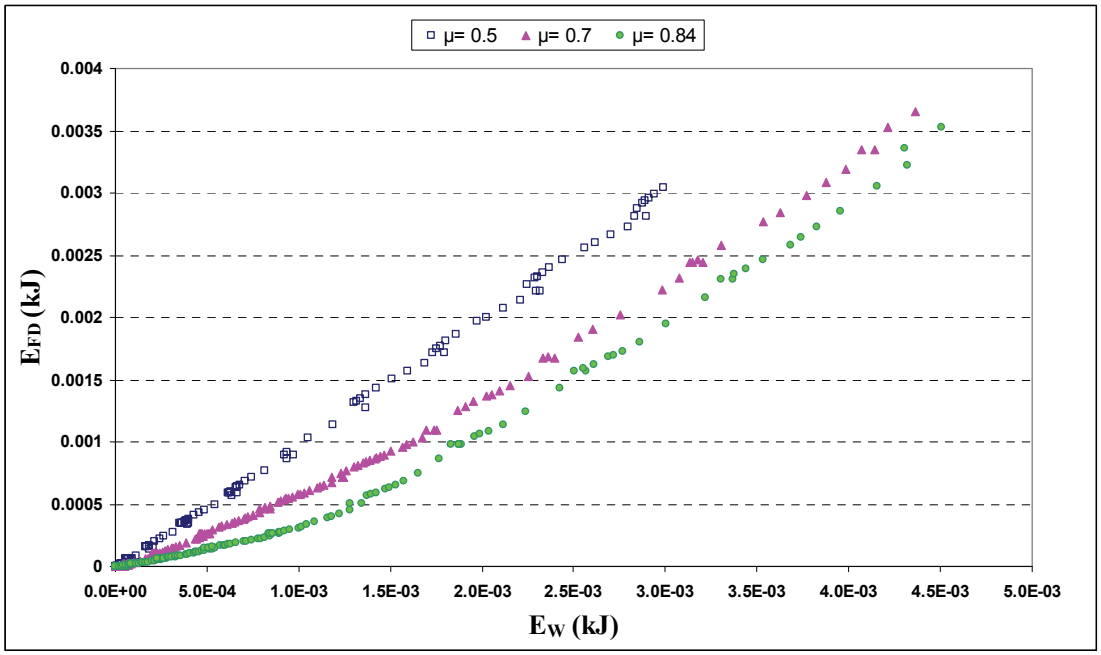

(a)

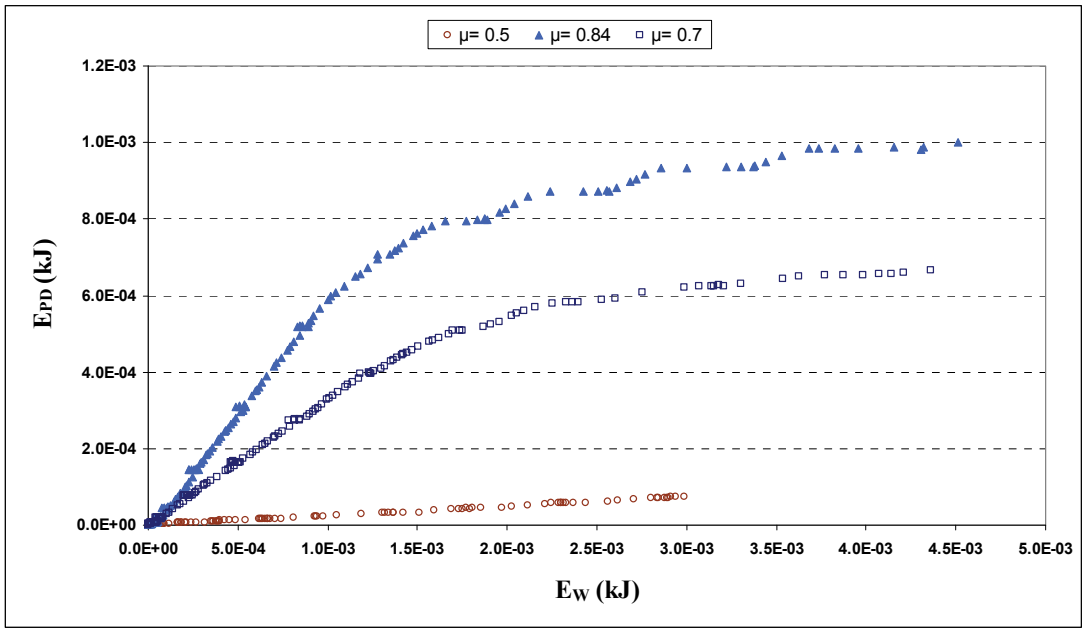

(b)

Fig 17. Variation of energy components (a) E_{FD} vs E_W, and (b) E_{PD} vs E_W for a soilbag assembly under cyclic loading.

Further analysis of the assembly of a soilbag provides supplementary details for the above-mentioned variation of energy components using E_{FD} - E_W and E_{PD} - E_W relationships for various friction coefficients (Fig 17).

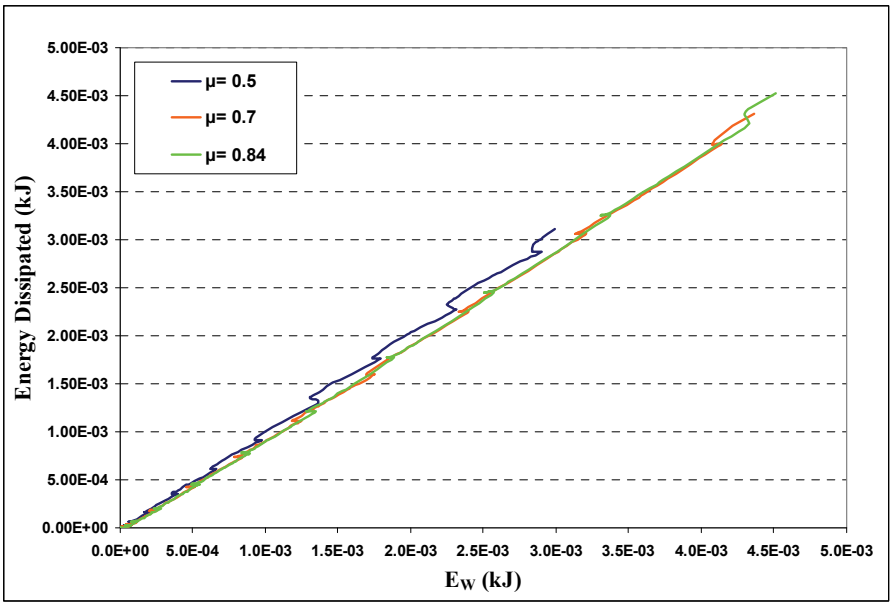

Fig 18. Variation of total dissipated energy of a soilbag under cyclic loading.

It is noticeable that the inelastic component of the energy for a soilbag assemblage, E_{PD} , under cyclic loading would increase with any particular increase in the tangential friction coefficient of the soil-bag interface while predictably, the frictional part of the total dissipated energy would decrease with similar variation in the frictional coefficient μ . However, as illustrated in Fig.18, the variation of total dissipated energy of a soilbag assemblage ($E_{PD} + E_{FD}$) under cyclic loading is somewhat linear while its magnitude is rather independent of the value of friction coefficient of a soil-bag interface.

CONCLUSIONS

The mechanical behaviour of the assembly of a soilbag subject to vertical (compression) loading and horizontal cyclic (simple shear) loading has been studied numerically by taking into account the active contact kinematic constraints at the soil-bag interface. Large-deformation frictional contact between the granular material (sand) and wrapping material (bag) is modelled using the master surface/slave surface penalty method formulation. Two and three dimensional models are presented in order to simulate the assemblage of the soilbag using the commercial finite element code 'ABAQUS' for its practical 3D mesh generation algorithms as well as its computational efficiency throughout large deformation contact mechanics simulations. To overcome the convergence difficulty, special care has been taken to ensure appropriate model discretisation and element type selection, and to ensure mesh dimensions as well as contact discretisation are adequate (Table 1).

As expected, it is shown that the stiffness and compression capacity of the assembly of a soilbag are considerably higher than those of the granular material while unwrapped. By introducing a frictional contact, separation and reclosure of the soil-bag interface has been considered during the analysis of the mechanical behaviour of a soilbag under different loading conditions. A brief study on the evolution of different energy components within the structure of a sandbag under cyclic loading indicated that though the magnitude of different energy dissipation components vary with the friction coefficient of the soil-bag interface, the variation of total dissipated energy with respect to the friction angle is rather insignificant.

REFERENCES

ABAQUS/Standard User's Manual, Version 6.7, Hibbitt, Karlsson & Sorensen; 2001.

Aqil, U., Matsushima, K., Mohri, Y., Yamazaki, S., and Tatsuoka, F. "Lateral shearing tests on geosynthetic soil bags." *8th International Conference on Geosynthetics*, Yokohama, Japan, 1703–1706.

Aqil, U., Matsushima, K., Mohri, Y., Yamazaki, S., and Tatsuoka, F. "Failure mechanism of geosynthetic soil bags in lateral
shearing." *Proceedings of the 41st Annual Symposium on Geotechnical Engineering*, Kagoshima, Japan, 687-688.

Argyris, J., Faust, G., Szimmat, J., Warnke, E. P., and William, K. J. (1974). "Recent developments in the finite element analysis of PCRV." 2nd Int. Conf. SMIRT, Nuclear Engineering and Design, Berlin, 42-75.

Barber, J. R., and Ciavarella, M. (2000). "Contact mechanics." *International Journal of Solids and Structures*, 37(1-2), 29-43.

Huang, C.-C., Matsushima, K., Mohri, Y., and Tatsuoka, F. (2008). "Analysis of sand slopes stabilized with facing of soil bags with extended reinforcement strips." *Geosynthetics International*, 15(4), 232-245.

Krahn, T., Blatz, J., Alfaro, M., and Bathurst, R. J. (2007). "Large-scale interface shear testing of sandbag dyke materials." *Geosynthetics International*, 14(2), 119-126.

Kubo, T., Yokota, Y., Ito, S., Matsuoka, H., and Liu, S. H. "Trial construction and behaviors of an arching structure with large-sized soilbags." *Proceedings of the 36th Japan National Conference on Geotechnical Engineering*, 2099-2100.

Lade, P. V., and Duncan, J. M. (1975). "Elastoplastic Stress-Strain Theory for Cohesionless Soil." *Geotechnical Engineering Division, ASCE*, 101, 1037-1053.

Lambe, T. W., and Whitman, R. V. (1979). *Soil Mechanics*, Wiley, New York.

Lohani, T. N., Matsushima, K., Aqil, U., Mohri, Y., and Tatsuoka, F. (2006). "Evaluating the strength and deformation characteristics of a soil bag pile from full-scale laboratory tests." *Geosynthetics International*, 13(6), 246-264.

Matsuoka, H. (2003). "Tribology in soilbag." *Journal of Japanese Society of Tribologists*, 48(7), 547-552.

Matsuoka, H., Hasebe, T., Liu, S. H., and Shimao, R. "Friction property of soilbags and some measures to increase soil bag resistances against sliding." *Proceedings of the 38th Annual Symposium on Geotechnical Engineering*, Akita, Japan, 869-870.

Matsuoka, H., Hasebe, T., Liu, S. H., and Shimao, R. (2004a). "Deformation-strength properties and design methods of soilbag assembly." *Journal of Geotechnical Engineering, JSCE*, 67(764), 169-181.

Matsuoka, H., and Liu, S. (2006). *A new earth reinforcement method using soilbags*, Taylor & Francis, London.

Matsuoka, H., and Liu, S. H. (2003). "New earth reinforcement method by soilbags ("donow")." *Soils and Foundations*, 43(6), 173-188.

Matsuoka, H., Liu, S. H., and Yamaguchi, K. "Mechanical properties of soilbags and their application to earth reinforcement." *Proceedings of the International Symposium on Earth Reinforcement*, Fukuoka, Japan, 587-592.

Matsuoka, H., Muramatsu, D., Liu, S. H., and Inoue, T. (2004b). "Reduction of environment ground vibration by soilbags." *Journal of Geotechnical Engineering, JSCE*, 67(764), 235-245.

Matsuoka, H., and Nakai, T. "Stress-deformation and strength characteristics of soil under three different principal stresses." *Proceedings of JSCE*, 59-74.

Matsushima, K., Aqil, U., Mohri, Y., and Tatsuoka, F. (2008). "Shear strength and deformation characteristics of geosynthetic soil bags stacked horizontally and inclined." *Geosynthetics International*, 15(2), 119-135.
Matsushima, K., Lohani, T. N., Aqil, U., Mohri, Y., and Yamazaki, S. "Study on compression characteristics of geosynthetics soilbags: applicability in small earth fill dams." *Proceedings of the 20th Geosynthetics Symposium*, Tokyo, Japan, 101-108.
Merifield, R., White, D. J., and Randolph, M. F. (2008). "The ultimate undrained resistance of partially embedded pipelines." *Ge´otechnique*, 58(6), 461-470.
Muramatsu, D., Zhang, F., and Shahin, H. M. (2007). "Numerical Simulation on Bearing Capacity of soilbag-reinforced Ground considering Finite Deformation." *Japanese Geotechnical Journal* 2(1), 11-23.
Muramatsu, M., Bin, Y., and Zhang, F. (2009). "Numerical Simulation of Vibration Damping Effect of soilbag." *Japanese Geotechnical Journal*, 4(1), 71-80.
Nakai, T., and Hinokio, M. (2004). "A simple elastoplastic model for normally and over consolidated soils with unified material parameters." *Soils and Foundations*, 44, 53-70.
Randolph, M. F., Wang, D., Zhou, H., Hossain, M. S., and Hu, Y. (2008). "Large Deformation Finite Element Analysis for Offshore Applications." 12th International Conference of International Association for Computer Methods and Advances in Geomechanics (IACMAG), Goa, India.
Sheng, D., Eigenbrod, K. D., and Wriggers, P. (2005). "Finite element analysis of pile installation using large-slip frictional contact." *Computers and Geotechnics*, 32(1), 17-26.
Sheng, D., and Sloan, S. W. (2000). "Aspects of finite element implementation of critical state models." *Computational Mechanics*, 2(26), 185-196.
Sheng, D., Sun, D. A., and Matsuoka, H. (2006). "Cantilever sheet-pile wall modelled by frictional contact." *Soils and Foundations*, 46(1).
Sheng, D., Wriggers, P., and Sloan, S. W. (2007). "Application of Frictional Contact in Geotechnical Engineering." *International Journal of Geomechanics*, 7(3), 176-185.
Suzuki, T., Yamashita, S., Matsuoka, H., and Yamaguchi, K. "Effect of wrapped gravel on prevention of frost heaving." *the 35th Japan National Conference on Geotechnical Engineering*, Japan, 609-610.
Tantono, S. F., and Bauer, E. (2008). "Numerical simulation of a soilbag under vertical compression." The 12th International Conference of International Association for Computer Methods and Advances in Geomechanics (IACMAG), Goa, India.
Tatsuoka, F. (2004). "An approximate isotropic perfectly plastic solution for compressive strength of geosynthetic-reinforced soil." *Geosynthetic International*, 11(5), 390-405.
Tatsuoka, F., Tateyama, M., Uchimura, T., and Koseki, J. (1997). "Geosynthetic-Reinforced Soil Retaining Walls as Important Permanent Structures." *Geosynthetic International*, 4(2), 81-136.
Wriggers, P. (2002). *Computational Contact Mechanics*, Wiley & Sons, Berlin, Heidelberg.
Xu, Y. F., Huang, H., Du, Y. J., and Sun, D. A. (2008). "Earth reinforcement using soilbags." *Geotextiles and Geomembranes*, 26(3), 279-289.
Xu, Y. F., and Huang, J. (2009). *Case Study on Earth Reinforcement Using Soilbags* Springer Berlin Heidelberg, Shanghai, China.
Yamamoto, H., Matsuoka, H., simao, R., Hasebe, T., and Hattori, M. "Cyclic Shear Property and damping ratio of soilbag assembly." *Processdings of the 38th Japan National Conference on Geotechnical Engineering*, 757-758.